
Cytostatic and Pro-Apoptotic Effects of *Justicia spicigera* Schltdl. on LNCaP Prostate Cancer Cells: Role of G₀/G₁ Cell Cycle Arrest and Phytochemical Characterization

Ivette Bravo-Espinoza , [Fabiola Hernández-Rosas](#) , [María Elena Hernández-Aguilar](#) ,
Marycarmen Godínez-Victoria , [Rodrigo Rafael Ramos-Hernández](#) , [Carlos Alberto López-Rosas](#) ,
[Santiago González-Periañez](#) , [Ezri Cruz-Pérez](#) , [Fernando Rafael Ramos-Morales](#) * , [Tushar Janardan Pawar](#) *

Posted Date: 22 January 2026

doi: 10.20944/preprints202506.2064.v2

Keywords: *Justicia spicigera*; muicle; LNCaP cells; prostate cancer; kaempferitrin; apoptosis; cell cycle arrest; Mexican ethnomedicine



Preprints.org is a free multidisciplinary platform providing preprint service that is dedicated to making early versions of research outputs permanently available and citable. Preprints posted at Preprints.org appear in Web of Science, Crossref, Google Scholar, Scilit, Europe PMC.

Copyright: This open access article is published under a [Creative Commons CC BY 4.0 license](#), which permit the free download, distribution, and reuse, provided that the author and preprint are cited in any reuse.

Disclaimer/Publisher's Note: The statements, opinions, and data contained in all publications are solely those of the individual author(s) and contributor(s) and not of MDPI and/or the editor(s). MDPI and/or the editor(s) disclaim responsibility for any injury to people or property resulting from any ideas, methods, instructions, or products referred to in the content.

Article

Cytostatic and Pro-Apoptotic Effects of *Justicia spicigera* Schltdl. on LNCaP Prostate Cancer Cells: Role of G₀/G₁ Cell Cycle Arrest and Phytochemical Characterization

Ivette Bravo-Espinoza ^{1,2}, Fabiola Hernandez-Rosas ^{3,4}, María Elena Hernández-Aguilar ², Marycarmen Godínez-Victoria ⁵, Rodrigo Rafael Ramos-Hernández ⁶, Carlos Alberto López-Rosas ^{1,6}, Santiago González-Periañez ⁶, Ezri Cruz-Pérez ¹, Fernando Rafael Ramos-Morales ^{1,6,*} and Tushar Janardan Pawar ^{7,8,*}

¹ Facultad de Química Farmacéutica Biológica, Universidad Veracruzana, Circuito Gonzalo Aguirre Beltrán s/n, Zona Universitaria, 91090 Xalapa-Enríquez, Veracruz, México

² Instituto de Investigaciones Cerebrales, Universidad Veracruzana, Luis Castelazo Ayala s/n, Col. Industrial Animas, 91190 Xalapa-Enríquez, Veracruz, México

³ Centro de Investigación, Universidad Anáhuac Querétaro, El Marqués, Querétaro 76246, Mexico

⁴ Facultad de Química, Universidad Autónoma de Querétaro, Querétaro 76010, Mexico

⁵ Sección de Estudios de Posgrado e Investigación, Escuela Superior de Medicina, Instituto Politécnico Nacional, Mexico City, Mexico

⁶ Instituto de Química Aplicada, Universidad Veracruzana, Luis Castelazo Ayala s/n, Col. Industrial Animas, 91190 Xalapa-Enríquez, Veracruz, México

⁷ Dirección de mecatrónica, Universidad Politécnica de Querétaro, Carretera estatal 420 S/N, El Rosario, 76240, Querétaro, México

⁸ Escuela de Ingeniería Química, Universidad Anáhuac Querétaro, Circuito Universidades I, Fracción 2 S/N, Zibatá, El Marqués, 76246, Querétaro, Mexico

* Correspondence: frames@uv.mx (F.R.R.M.); tushar.pawar@anahuac.mx (T.J.P.)

Abstract

Justicia spicigera is a central medicinal plant in Mexican ethnomedicine, yet its therapeutic potential against prostate cancer remains largely unexplored. This study investigated the antiproliferative and pro-apoptotic effects of a 50% hydroalcoholic extract from the leaves and stems of *J. spicigera* on androgen-sensitive LNCaP prostate cancer cells. Phytochemical profiling via TLC and LC-MS putatively identified the bioactive flavonoid kaempferitrin within the complex extract. Biological assays, including MTT, trypan blue exclusion, and flow cytometry, revealed that the extract inhibits LNCaP proliferation in a distinct, dose-dependent manner. At a lower concentration (250 µg/mL), the extract exerted a primarily cytostatic effect by inducing significant G₀/G₁ cell cycle arrest without triggering immediate cell death. Conversely, higher concentrations (≥500 µg/mL) were potentially cytotoxic, reducing cell viability to below 20% and inducing late apoptosis in approximately 58% of the population within 24 hours. These results validate the biological activity of *J. spicigera* in a prostate cancer model and suggest that the extract, or its constituent flavonoids could serve as a template for developing treatments that target both cell cycle checkpoints and programmed cell death.

Keywords: *Justicia spicigera*; muicle; LNCaP cells; prostate cancer; kaempferitrin; apoptosis; cell cycle arrest; Mexican ethnomedicine

1. Introduction

Prostate cancer (PCa) is one of the most frequently diagnosed malignancies in men and remains a primary driver of cancer-related mortality globally [i,ii]. Along with benign prostatic hyperplasia (BPH), these conditions represent a substantial burden for patients and healthcare systems, particularly in Mexico. In 2023, Mexico recorded 7,241 deaths from prostate cancer, reflecting a mortality rate of 34.6 per 100,000 men over the age of 40. For 2024, the incidence rate was reported at 28.9 per 100,000 men in the same age group, totaling 6,050 new cases. The prevalence of non-malignant disease is even more pronounced; BPH accounted for 123,215 new cases in 2024, an incidence rate of 589.4 per 100,000 men (INEGI, 2025; SSA, 2025). PCa is a highly heterogeneous disease that progresses through localized, advanced, and metastatic stages, each requiring specific therapeutic interventions [iii,iv,v]. While environmental factors and genetic predisposition influence onset, mutations in genes such as BRCA1, BRCA2, and TP53, which regulate DNA repair and androgen metabolism significantly contribute to disease progression [vi].

The androgen receptor (AR) signaling pathway is the central axis of PCa biology and a primary therapeutic target. Conventional strategies, including androgen deprivation therapy (ADT), chemotherapy, and immunotherapy, have shown clinical efficacy; however, the development of drug resistance and treatment-associated toxicities underscore the urgent need for alternative or complementary approaches [vii]. Historically, traditional medicine has been a cornerstone of cancer therapy, with medicinal plants serving as essential sources of bioactive compounds for drug discovery. In Mexico, species such as 'cuachalalate' (*Amphipterygium adstringens*) are used for inflammatory conditions, while soursop (*Annona muricata*) is utilized for its reputed antitumor properties [viii,ix]. Additionally, species of the genus *Verbesina* have gained scientific attention for their bioactive secondary metabolites and traditional use in treating neoplastic conditions, further illustrating the therapeutic potential of the Mexican flora [x,xi].

The importance of natural products in modern oncology is further highlighted by the fact that several FDA-approved agents, including paclitaxel, vinblastine, and camptothecin, are derived from these sources [xii]. These limitations underscore the need for alternative strategies, including the use of medicinal plants that offer low toxicity and broader accessibility. *Justicia spicigera*, a plant widely used in Mexican ethnomedicine, has attracted scientific interest. In Mexican ethnomedicine, it has been widely utilized for treating anemia, menstrual irregularities, respiratory diseases, and microbial infections [xiii,xiv,xv]. Its diverse bioactive compounds, primarily from the leaves and aerial parts, including various flavonoids and anthocyanins, are known to exhibit anticancer, anti-inflammatory, and immunomodulatory properties [xvi,xvii,xviii]. While previous studies have reported that kaempferitrin, a key flavonoid in *J. spicigera*, induces apoptosis in various cancer models, its precise effects on prostate cancer cells remain largely unexplored. Given that prostate cancer treatment resistance is often linked to evasion of apoptosis, investigating whether *J. spicigera* influences cell cycle progression or apoptotic pathways in LNCaP cells is essential. Many plant-derived compounds influence cancer progression by modulating the cell cycle, inducing apoptosis, or targeting signaling pathways central to tumor survival and proliferation.

The Acanthaceae family, to which *Justicia spicigera* Schltld., commonly known as "muicle," belongs, includes more than 600 species used in traditional medicine for various ailments, including inflammation, infections, and metabolic disorders [xix,xx]. However, despite its broad therapeutic applications, research on the potential anticancer effects of *J. spicigera* remains limited. Several studies have reported the presence of flavonoids, phytosterols, and terpenoids in *J. spicigera*, many of which exhibit promising anticancer properties [xxi,xxii,xxiii,xxiv]. Kaempferitrin and quercetin derivatives, found in *J. spicigera*, have demonstrated antiproliferative and apoptotic activity, acting through the modulation of p53, Bcl-2, Bax, and cyclins, which regulate cell cycle progression and programmed cell death [xxv]. Additionally, β -sitosterol, a major phytosterol in *J. spicigera*, has been shown to inhibit prostate cancer cell proliferation by modulating ceramide metabolism and AR signaling [xxvi].

Although the cytotoxic effects of an extract from the leaves of *J. spicigera* have been reported in leukemia (TF-1), cervical (HeLa), and breast (T47D) cancer cells [xxvii,xxviii], its potential cytotoxic

effect in prostate cancer, particularly in androgen-sensitive models like LNCaP, remains largely unexplored. Previous studies have demonstrated that an extract from the leaves of *J. spicigera* induces apoptosis at low micromolar concentrations, with IC_{50} values as low as 17 $\mu\text{g}/\text{mL}$ in HeLa cells [xxix]. Additionally, an in vivo study showed that *J. spicigera* extract suppressed tumor growth by up to 53%, comparable to the effects of cisplatin, suggesting significant anticancer potential [xxx].

One of the major challenges in prostate cancer therapy is overcoming drug resistance and systemic toxicity associated with conventional treatments [xxxi]. Many standard chemotherapeutics exert their effects by inducing direct cytotoxicity, leading to significant side effects and the selection of resistant cancer cell populations. In contrast, cytostatic agents, which inhibit cell proliferation without immediately triggering apoptosis, offer an alternative approach that may delay tumor progression and reduce therapy resistance [xxxii].

Given the growing interest in plant-derived cytostatic compounds, it is critical to investigate whether *J. spicigera* primarily acts via cell cycle modulation or through direct apoptosis induction. The presence of flavonoids and sterols in *J. spicigera* suggests a possible mechanism involving G_0/G_1 arrest and subsequent apoptosis induction, as previously demonstrated in other plant-derived anticancer compounds [xxx]. However, no study has comprehensively evaluated these effects in prostate cancer models, warranting further investigation.

Despite preliminary evidence of anticancer activity, studies assessing *J. spicigera* in prostate cancer models, especially in androgen-responsive LNCaP cells remain scarce. A prior study reported that a hydroalcoholic extract from the aerial parts of *J. spicigera* induced a modest G_0 -phase cell cycle arrest in LNCaP cells at high concentrations ($IC_{50} = 3026 \pm 421 \mu\text{g}/\text{mL}$) but lacked significant apoptotic effects [xxxiii]. The limited apoptotic response observed in earlier studies prompts a closer examination of whether *J. spicigera* can activate programmed cell death pathways at lower, therapeutically relevant concentrations, an aspect that has not been thoroughly addressed to date. Therefore, this study aimed to investigate the antiproliferative effects of a hydroalcoholic extract of *J. spicigera* on LNCaP prostate cancer cells by characterizing its phytochemical composition, determining its dose-dependent cytostatic and cytotoxic activity, and elucidating its impact on cell cycle progression and apoptosis.

2. Results

2.1. Phytochemical Profiling of *J. spicigera* Extract

The phytochemical composition of the *J. spicigera* extract was investigated using chromatographic and mass spectrometric techniques, as summarized in Figure 1. The analysis suggests the presence of the flavonoid kaempferitrin [xvi]. Preliminary screening by analytical thin-layer chromatography (TLC) indicated the presence of flavonoids in the extract. When developed with a flavonoid-specific reagent, a prominent spot was observed with strong fluorescence under UV 365 nm light (Figure 1A) [xxii,xxx].

To further investigate the composition, the extract was analyzed by Liquid Chromatography-Mass Spectrometry (LC-MS). The Total Ion Chromatogram (TIC) revealed a complex mixture containing multiple components, with major, unidentified compounds eluting at approximately 7.5 min and 13.3 min (Figure 1B, marked with asterisks). Based on literature reports of flavonoids in *J. spicigera*, the data was searched for the mass corresponding to kaempferitrin. The Extracted Ion Chromatogram (EIC) for its protonated molecule ($[M+H]^+$, m/z 579.1) showed a distinct peak at a retention time of approximately 6.8 minutes (Figure 1C). The mass spectrum of this peak confirmed an ion at m/z 579.1563. This observed mass corresponds closely to the calculated exact mass for the kaempferitrin $[M+H]^+$ ion (579.1714), supporting its putative identification in the extract (Figure 1D) [xxv].

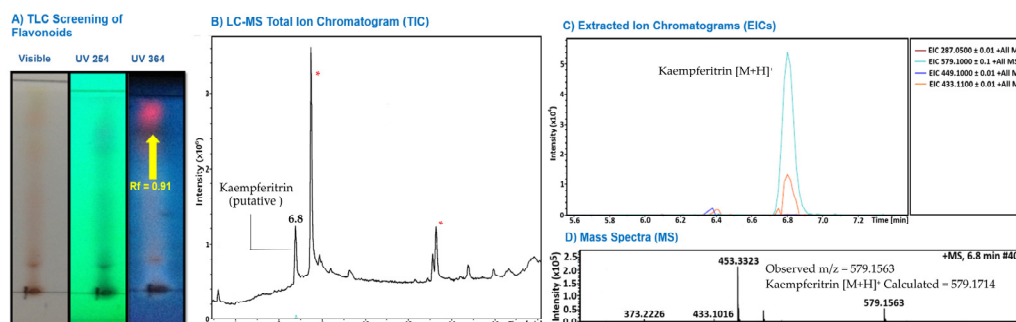


Figure 1. Preliminary phytochemical characterization of the hydroalcoholic extract of *J. spicigera* leaves and stems. (A) Preliminary TLC analysis developed with 1% aluminum chloride and visualized under UV 365 nm light. The arrow indicates a spot ($R_f = 0.91$) with fluorescence characteristic of the flavonoid class. (B) LC-MS Total Ion Chromatogram (TIC) showing the overall profile of the extract. The arrow indicates the peak putatively identified as kaempferitrin ($t_R \approx 6.8$ min). Major, unidentified components are marked with an asterisk (*). (C) Extracted Ion Chromatograms (EICs) for key masses. The cyan trace shows a distinct peak for the ion at m/z 579.1, corresponding to the putative $[M+H]^+$ of kaempferitrin, at 6.8 min. (D) Mass spectrum from the peak at 6.8 min, showing the observed parent ion $[M+H]^+$ at m/z 579.1563, which corresponds closely to the calculated mass for kaempferitrin ($C_{27}H_{31}O_{14}^+$, 579.1714).

2.2. Effects of *J. spicigera* on LNCaP Cell Proliferation

To investigate the antiproliferative effects of *J. spicigera* extract, a combination of colorimetric and microscopic assays was used to assess cell viability, morphology, and membrane integrity. The results demonstrated a dose- and time-dependent inhibition of LNCaP cell proliferation, with evidence of cytostatic effects at sub-lethal concentrations and cytotoxic responses at higher doses.

2.2.1. MTT Assay

The metabolic activity of LNCaP cells was evaluated using the MTT assay after exposure to increasing concentrations of *J. spicigera* extract (62.5–4000 $\mu\text{g/mL}$) for 24, 48, and 72 h. At 250 $\mu\text{g/mL}$, no significant reduction in viability was observed at 24 h, suggesting minimal cytotoxicity at this concentration. However, at 500 $\mu\text{g/mL}$, a marked reduction in cell viability was detected ($p < 0.001$), which became more pronounced at extended time points. At higher concentrations (1000–4000 $\mu\text{g/mL}$), viability decreased to below 20% by 72 h, closely resembling the effect of the positive control etoposide (10 μM) (Figure 2).

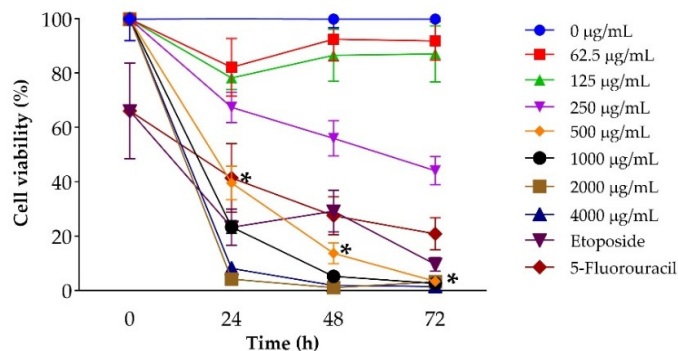


Figure 2. Effect of *J. spicigera* extract on LNCaP cell viability. Cells were treated with increasing concentrations of the extract for 24, 48, and 72 hours. Cell viability was assessed by the MTT assay and is expressed as a percentage relative to the untreated control (0 $\mu\text{g/mL}$), which is set at 100%. Values are presented as mean \pm SEM ($n = 9$). * $p < 0.001$ compared to the untreated control.

2.2.2. Morphological Characterization of Treated LNCaP Cells

To complement the metabolic viability data, phase-contrast microscopy was performed to assess the morphological changes induced by the extract. Untreated control cells maintained a polygonal epithelial morphology with dense, adherent colonies typical of LNCaP cells. Following treatment with 250 $\mu\text{g}/\text{mL}$ extract, cells exhibited slight reductions in colony density and spreading at 48 h, without evidence of membrane disruption or blebbing, findings consistent with a cytostatic response. In contrast, cells exposed to 500 $\mu\text{g}/\text{mL}$ showed early signs of apoptosis as early as 24 h, including cell shrinkage, rounding, and partial detachment from the substrate. These changes intensified at 48 h, marked by pronounced membrane blebbing and disruption of the monolayer (Figure 3).

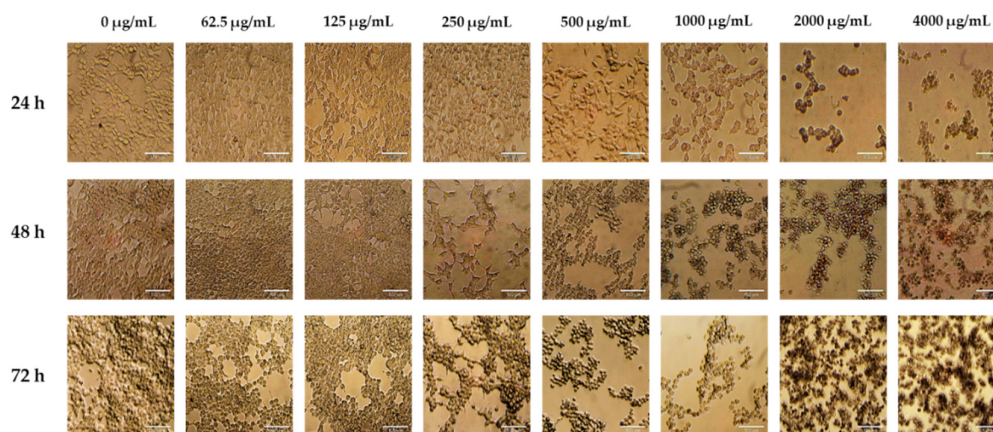


Figure 3. Morphological analysis of LNCaP cells treated with *J. spicigera* extract at 250 and 500 $\mu\text{g}/\text{mL}$ for 24 h, 48 h and 72 h. Representative phase-contrast micrographs demonstrate dose- and time-dependent morphological changes, including cell rounding, detachment, and reduced adherence. Scale bar = 100 μm .

2.2.3. Trypan Blue Assay

To directly assess membrane integrity and distinguish viable from non-viable cells, the trypan blue exclusion assay was conducted under the same treatment conditions. At 250 $\mu\text{g}/\text{mL}$, no significant reduction in viable cell counts was observed at 24 h, while a modest but significant decline emerged by 48 h ($p < 0.05$), consistent with delayed cytostatic effects. At 500 $\mu\text{g}/\text{mL}$, viability dropped sharply at 48 and 72 h ($p < 0.001$), corroborating the cytotoxic threshold observed in MTT (Figure 4A) and morphological analyses (Figure 4B).

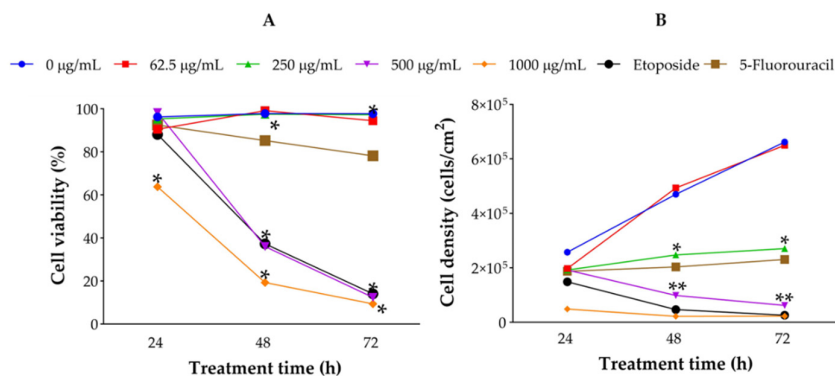


Figure 4. Trypan blue exclusion assay results showing viable and non-viable LNCaP cells after treatment with *J. spicigera* extract at 24, 48, and 72 hours. Values represent mean \pm SEM ($n = 9$). Statistical significance: (* $p < 0.05$, ** $p < 0.001$).

2.3. Apoptosis Induction and Cell Viability

J. spicigera extract induced apoptosis in LNCaP cells in a dose-dependent manner, as determined by Annexin V/PI staining and flow cytometry analysis (Figure 5). At 250 $\mu\text{g/mL}$, the percentage of apoptotic cells remained comparable to that of untreated controls, confirming that this concentration primarily exerts a cytostatic rather than cytotoxic effect. However, at 500 $\mu\text{g/mL}$, a significant increase in early apoptosis was observed at 24 h, progressing to late apoptosis at 48 h ($p < 0.001$ vs. control). At concentrations of 1000 $\mu\text{g/mL}$ and above, apoptosis was predominant, with a concurrent increase in necrotic cell death, similar to the effect observed with etoposide (positive control).

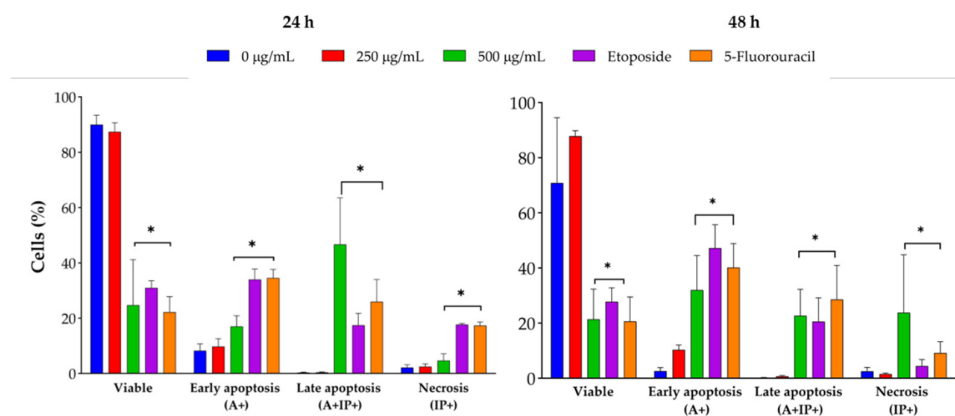


Figure 5. Flow cytometry analysis of LNCaP cells treated with *J. spicigera* extract at 250, 500, and 1000 $\mu\text{g/mL}$ for 24 and 48 hours. Apoptotic cells were detected using Annexin V/PI staining. Bars represent mean \pm SEM ($n = 3$). (* $p < 0.001$).

The dot plots showing Annexin V/PI staining at 24 and 48 h provide visual confirmation of the dose-dependent shift from viability to apoptosis (Figure 6 and 7). At 24 h, a shift from viable to apoptotic quadrants was evident at ≥ 500 $\mu\text{g/mL}$. At 48 h, this shift was more pronounced, with the highest concentrations inducing widespread late apoptosis and necrosis, while 250 $\mu\text{g/mL}$ maintained a largely viable profile.

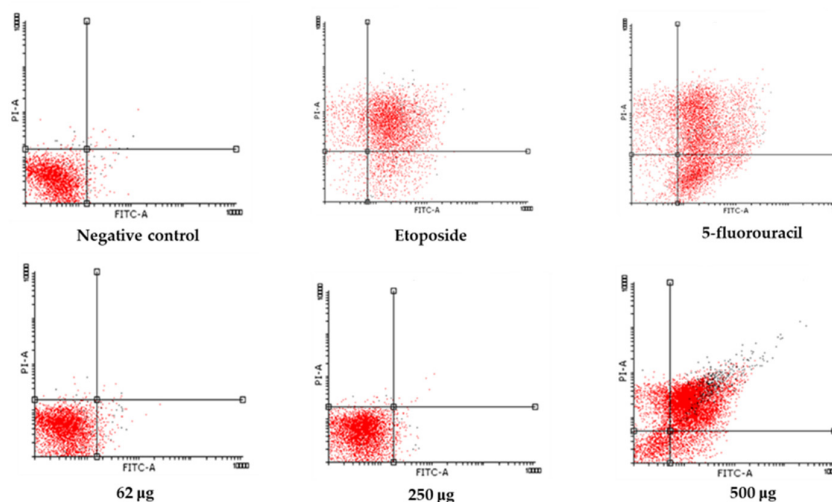


Figure 6. Annexin V-FITC/PI dot plots of LNCaP cells at 24 h. Treatments include control, 62.5 $\mu\text{g/mL}$, 250 $\mu\text{g/mL}$, 500 $\mu\text{g/mL}$, and positive controls (etoposide and 5-fluorouracil). Apoptotic populations shift toward the lower-right and upper-right quadrants in a dose-dependent manner.

To further distinguish between viable and non-viable cells, flow cytometry with propidium iodide (PI) exclusion was conducted (Figure 8). At 250 $\mu\text{g/mL}$, the percentage of viable cells remained above 85% at both 24 and 48 h. In contrast, at 500 $\mu\text{g/mL}$, a significant reduction in viable cell populations was observed by 48 h, with a notable increase in apoptotic cells ($p < 0.001$). At 1000 $\mu\text{g/mL}$, cell viability dropped dramatically, with a substantial transition to late apoptosis or necrosis.

Collectively, the flow cytometry and viability data indicate that apoptosis is the predominant mode of cell death at concentrations ≥ 500 $\mu\text{g/mL}$, while the 250 $\mu\text{g/mL}$ concentration primarily maintains membrane integrity and cell viability.

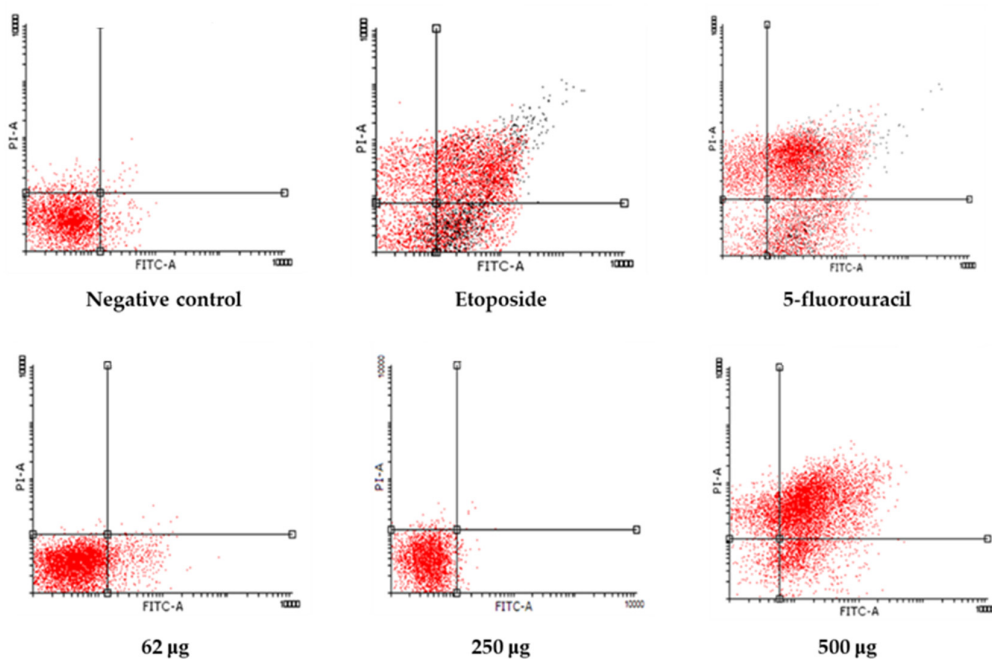


Figure 7. Annexin V-FITC/PI dot plots of LNCaP cells at 48 h. Apoptotic and necrotic populations increase with extract concentration and are most pronounced at 500 $\mu\text{g/mL}$ and 1000 $\mu\text{g/mL}$. Positive controls show widespread cell death, while 250 $\mu\text{g/mL}$ retains a predominantly viable profile.

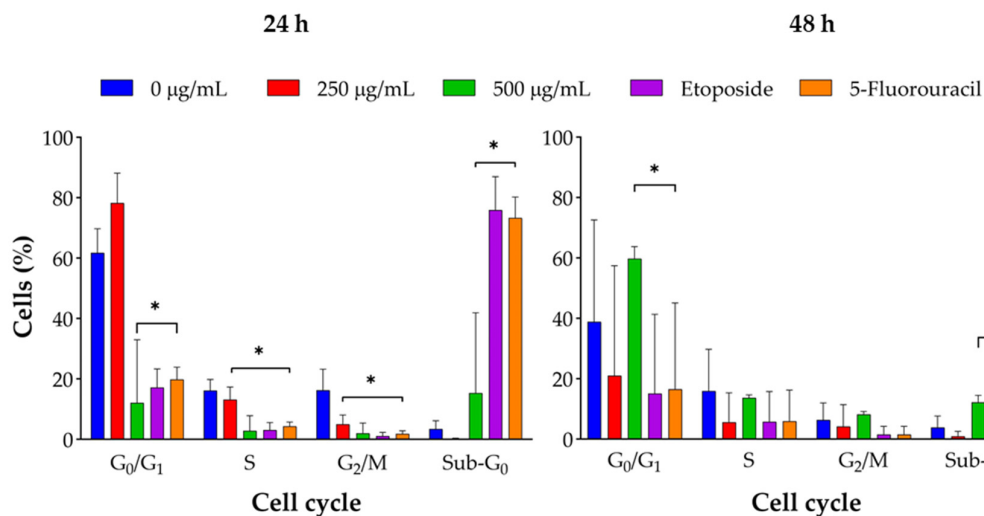


Figure 8. *J. spicigera* extract induces G_0/G_1 cell cycle arrest in LNCaP cells. Cells were treated with the indicated concentrations for 24 hours (left panel) and 48 hours (right panel). Cell cycle distribution was determined by

propidium iodide (PI) staining and flow cytometry. The graphs show the percentage of cells in the G_0/G_1 , S, G_2/M , and Sub- G_0 phases. Values are presented as mean \pm SEM ($n = 3$). * $p < 0.001$ compared to the corresponding control group.

2.4. Cell Cycle Arrest Mechanism

Flow cytometry analysis indicated that *J. spicigera* extract induced dose-dependent changes in the cell cycle distribution of LNCaP cells. At 250 $\mu\text{g/mL}$, a significant accumulation of cells in the G_0/G_1 phase was observed, alongside a reduction in the S phase population ($p < 0.01$). This pattern intensified at 500 $\mu\text{g/mL}$, with increased G_0/G_1 arrest, further S phase depletion, and a notable rise in the sub- G_0/G_1 fraction, consistent with DNA fragmentation and the onset of apoptosis ($p < 0.001$). At 1000 $\mu\text{g/mL}$, the sub- G_0/G_1 population became dominant, indicating that apoptotic cell death supersedes cytostatic effects at higher concentrations.

3. Discussion

This study provides a foundational analysis of the antiproliferative effects of a hydroalcoholic extract of *J. spicigera* on LNCaP prostate cancer cells. Our results demonstrate that the extract modulates cell behavior in a distinct, concentration-dependent manner (Figure 9). At a lower concentration (250 $\mu\text{g/mL}$), the extract consistently induced G_0/G_1 cell cycle arrest without triggering significant apoptosis, indicating an interference with early cell cycle checkpoints. In contrast, higher concentrations (≥ 500 $\mu\text{g/mL}$) produced a clear cytotoxic response, characterized by the induction of apoptosis, phosphatidylserine translocation, and DNA fragmentation.

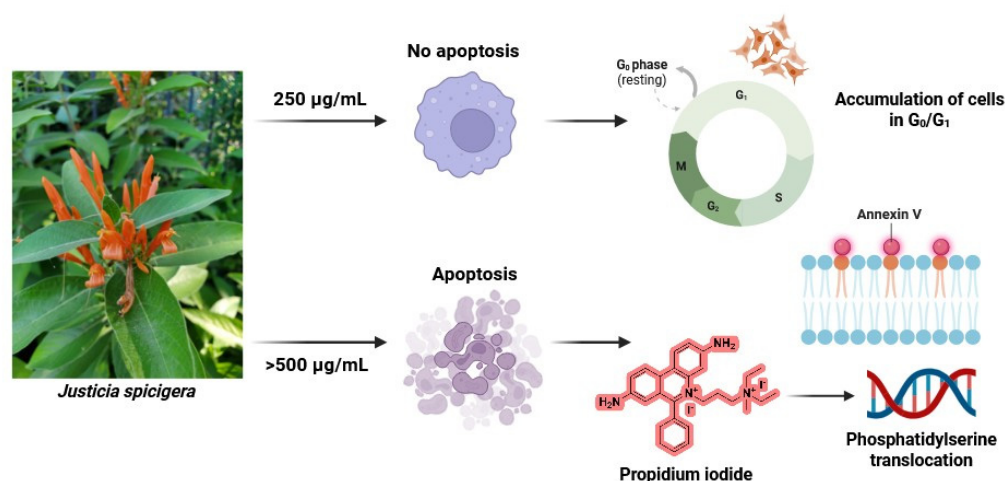


Figure 9. Proposed model of the dose-dependent effect of *J. spicigera* extract on LNCaP prostate cancer cells. At 250 $\mu\text{g/mL}$, the extract induces G_0/G_1 arrest, reducing proliferation without triggering apoptosis. At higher concentrations (≥ 500 $\mu\text{g/mL}$), it initiates apoptosis through phosphatidylserine translocation, caspase activation, and DNA fragmentation.

The mechanism behind these dual effects appears to be rooted in the extract's influence on cell cycle progression. The observed G_0/G_1 arrest points to a specific disruption of the molecular machinery governing the cell cycle's initial phase, likely through interference with regulators like cyclin D1/CDK4 [xxxiv,xxx,xxxv]. Our phytochemical analysis, which putatively identified the flavonoid kaempferitrin, provides a strong chemical basis for this activity. This is consistent with the known function of flavonoids, which characteristically target cell cycle regulators and DNA integrity pathways [xxv], and have been widely implicated in modulating crucial cancer-related pathways

such as PI3K/Akt, p53, and MAPK that directly influence cell cycle progression and survival [xxxvi,xxxvii].

As the concentration of the extract increases, the sustained pressure on the cell cycle likely pushes the cells toward programmed cell death. This transition from cytostasis to apoptosis aligns with reports of flavonoids and phytosterols modulating apoptotic signaling and mitochondrial function in cancer cells [xxviii,xxix]. The clear pattern of Annexin V positivity and sub-G₀/G₁ accumulation at concentrations ≥ 500 $\mu\text{g/mL}$ strongly suggests that this cytotoxicity is mediated by an activation of caspase-dependent apoptosis. Although the causative agent was not isolated, the putative identification of kaempferitrin further supports this hypothesis, as apoptosis induction has been previously linked to kaempferitrin and its analogs in other cancer models [xxxv,xxxvi,xxxvii,xxxviii,xxxix,xl,xli,xlii,xliii,xliv,xlv,xlvi].

When compared to previous reports, the cytotoxic potency of the *J. spicigera* extract on LNCaP cells, with a calculated IC₅₀ value of 236.8 $\mu\text{g/mL}$ at 72 hours, appears less potent than that observed in other cell lines; for instance, a prior study reported an IC₅₀ value of only 17 $\mu\text{g/mL}$ against HeLa cervical cancer cells [xxxiii]. This discrepancy may suggest a higher intrinsic resistance of LNCaP cells or a cell-line-specific sensitivity to the extract's constituents. However, the mechanism of G₀/G₁ arrest is consistent with the actions of other well-known, plant-derived agents against prostate cancer. Curcumin and epigallocatechin-3-gallate (EGCG), for example, have both been reported to inhibit LNCaP cell proliferation by inducing G₀/G₁ phase cell cycle arrest [xlvi]. Similarly, resveratrol has also been shown to inhibit LNCaP cell proliferation by inducing cell cycle arrest [xlviii]. The fact that the *J. spicigera* extract shares this mechanism highlights its potential as a relevant agent for controlling the growth of androgen-sensitive prostate cancer.

A significant finding of this study is the therapeutic implication of this dual, concentration-dependent mechanism. The selective induction of cell cycle arrest at lower, non-lethal doses suggests a more controlled, cytostatic profile. This contrasts with many conventional chemotherapeutics that exert immediate and often indiscriminate cytotoxicity, leading to significant side effects. Furthermore, compared to conventional chemotherapeutics that often cause G₂/M arrest, the preferential G₀/G₁ arrest observed with *J. spicigera* may offer a different point of intervention, particularly relevant to hormone-sensitive and AR-independent forms of prostate cancer [xlix].

While this study provides a strong rationale for the anticancer potential of *J. spicigera*, its limitations define clear directions for future research. The causative agent was not isolated, and the identification of kaempferitrin, while based on accurate mass, remains putative without definitive structural confirmation. Future work should focus on isolating this flavonoid to allow for unambiguous structural elucidation through spectroscopic methods like NMR. The most critical next step is to evaluate the extract's selectivity by testing its effects on non-malignant prostate epithelial cells, which is essential to determine its therapeutic window and potential for safe application. Furthermore, a deeper mechanistic validation through molecular assays targeting key regulators of the cell cycle (CDKs, Rb, p21) and apoptosis (Bcl-2, Bax, caspases) is warranted to delineate the precise pathways involved.

In conclusion, this study demonstrates that a hydroalcoholic extract of *J. spicigera* exerts a potent, dual-action antiproliferative effect on LNCaP prostate cancer cells, acting as a cytostatic agent at low concentrations and an apoptosis-inducing agent at higher concentrations. These findings provide the first detailed evidence supporting the potential use of this traditional Mexican medicinal plant for prostate cancer therapy and establish a strong scientific basis for future studies aimed at isolating its bioactive compounds and evaluating its efficacy and safety *in vivo*.

4. Materials and Methods

4.1. Plant Material and Extract Preparation

Fresh leaves and stems of *J. spicigera* were collected from Lencero, Veracruz, México (19° 29' 27.5" N, 96° 48' 53.6" W) in February 2021. The plant was taxonomically identified by Dr. Edison

Fernando Nicolalde-Morejón, a plant taxonomist at Universidad Veracruzana, and a voucher specimen (No. 15655) was deposited at the Herbarium of Instituto de Investigaciones Biológicas, Universidad Veracruzana, for future reference. The plant material was collected in compliance with national and international guidelines on biodiversity.

The collected plant material was washed with distilled water, air-dried at room temperature (25°C, 50–60% relative humidity) for seven days, and manually cut into small pieces. Hydroalcoholic extraction was performed by macerating 90 g of powdered plant material in 500 mL ethanol:water (50:50) at room temperature for 72 h with occasional stirring. The extract was filtered using Whatman No. 1 filter paper (Cytiva, Marlborough, MA, USA), concentrated under reduced pressure using a rotary evaporator (Büchi R-210, Flawil, Switzerland) at 40°C, and lyophilized in a freeze dryer (Labconco FreeZone 4.5, Kansas City, MO, USA) to obtain a dry extract. The hydroalcoholic extraction of 980 g of powdered plant material yielded 56 g of dry extract, corresponding to a yield of 5.71%.

4.2. Preliminary Phytochemical Characterization

The phytochemical composition of the *J. spicigera* hydroalcoholic extract was analyzed using TLC and LC-MS. Based on literature reports of its significant bioactivity, kaempferitrin was selected as a chemical marker for putative identification, although it was not the most abundant compound in the extract.

TLC was performed using silica gel 60 F254 plates (Merck, Darmstadt, Germany) as the stationary phase. The extract (5 µL) was applied as a spot and developed in a 1-butanol:water:acetic acid (6:3:1) solvent system. Plates were visualized under UV light (254 nm and 365 nm), followed by spraying with 1% aluminum chloride to detect flavonoids.

LC-MS analysis was performed on an Ultimate 3000 liquid chromatograph (Dionex Corp., Sunnyvale, CA, USA) coupled to a micrOTOF-Q II mass spectrometer (Bruker Daltonics, Billerica, MA, USA). Separation was performed on a C18 Hypersil column (5 µm, 250 × 4.6 mm). The mobile phase consisted of 0.01% formic acid in water (Solvent A) and acetonitrile (Solvent B), with a flow rate of 0.3 mL/min. The mass spectrometer was operated with an electrospray ionization (ESI) source in positive ion mode. The key parameters were: capillary voltage, 4500 V; nebulizer pressure, 1.6 Bar; dry gas flow, 12.0 L/min; and dry heater temperature, 200°C. The mass scan range was set from m/z 50 to 3000.

4.3. Cell Culture and Maintenance

The human prostate cancer cell line LNCaP (ATCC® CRL-1740™) was obtained from ATCC (Manassas, VA, USA) and maintained in RPMI-1640 medium (Gibco, Waltham, MA, USA) supplemented with 10% fetal bovine serum (FBS, Gibco, Waltham, MA, USA), 1% penicillin-streptomycin (Sigma-Aldrich, St. Louis, MO, USA), and 2 mM L-glutamine (Gibco, Waltham, MA, USA). Cells were incubated at 37°C in a humidified atmosphere with 5% CO₂ and passaged every 2–3 days upon reaching 70–80% confluence using 0.25% trypsin-EDTA (Gibco, Waltham, MA, USA).

Cell viability was monitored using the trypan blue exclusion assay, and only cultures with ≥95% viability were used for experiments. The absence of Mycoplasma contamination was routinely verified using a PCR-based Mycoplasma detection kit (Lonza, Basel, Switzerland).

For experimental treatments, LNCaP cells were seeded into 96-well, 12-well, or 6-well plates, depending on the assay requirements, and allowed to adhere for 24 h before treatment. Cells were then treated with varying concentrations of *J. spicigera* extract, while 0.1% DMSO served as the vehicle control (negative control).

4.4. MTT Assay for Cell Viability

The MTT assay was used to evaluate the effect of *J. spicigera* extract on LNCaP cell viability. This colorimetric assay measures the reduction of MTT into formazan crystals by mitochondrial dehydrogenases in metabolically active cells, with absorbance intensity correlating with the number of viable cells [1].

LNCaP cells were seeded in 96-well plates at 8×10^4 cells per well in 100 μL of RPMI-1640 medium and allowed to adhere for 24 h at 37°C in a 5% CO_2 incubator. After adherence, cells were treated with serial dilutions of *J. spicigera* extract (ranging from 62.5 to 4000 $\mu\text{g}/\text{mL}$) for 24, 48, and 72 h, with 0.1% DMSO serving as the vehicle control. Each condition was tested in triplicate wells across three independent experiments [li].

Following the incubation period, 10 μL of MTT (M2128, Sigma-Aldrich, St. Louis, MO, USA) solution (5 mg/mL in PBS, Sigma-Aldrich, St. Louis, MO, USA) was added to each well, and plates were incubated for 3 h at 37°C . The supernatant was removed, and 100 μL of DMSO (Sigma-Aldrich, St. Louis, MO, USA) was added to dissolve the formazan crystals. Absorbance was measured at 570 nm, with background correction at 650 nm, using a microplate reader (Multiskan GO, Thermo Fisher Scientific, Waltham, MA, USA). The assignment of different extract concentrations to the wells of the microplates was performed randomly.

Cell viability was calculated relative to the untreated control using the formula:

$$\text{Cell viability (\%)} = \frac{\text{Absorbance of treated cells}}{\text{Absorbance of control cells}} \times 100$$

4.5. Trypan Blue Exclusion Assay

The Trypan Blue exclusion assay was used to assess LNCaP cell viability following treatment with *J. spicigera* extract. This method differentiates between viable and non-viable cells, as intact plasma membranes exclude Trypan Blue, whereas compromised membranes allow dye uptake, making non-viable cells appear blue under a microscope [lii].

LNCaP cells were seeded in 12-well plates at 1×10^5 cells per well in 1 mL of RPMI-1640 medium (R8005, Sigma-Aldrich, St. Louis, MO, USA) and allowed to adhere for 24 h at 37°C in a humidified incubator with 5% CO_2 . After adherence, cells were treated with varying concentrations of *J. spicigera* extract (specifically 62.5, 250, 500, and 1000 $\mu\text{g}/\text{mL}$), with 0.1% DMSO as the vehicle control, 10 μM etoposide (Sigma-Aldrich, St. Louis, MO, USA) and 5-fluorouracil as the positive controls. Each condition was tested in triplicate wells across three independent experiments [li].

At the end of the incubation period, the culture medium was removed, and cells were trypsinized with 0.25% Trypsin-EDTA (Gibco, Waltham, MA, USA) for 2 min at 37°C . Trypsinization (T3924, Sigma-Aldrich, St. Louis, MO, USA) was halted by adding an equal volume of complete RPMI-1640 medium (10% FBS), and cells were resuspended in PBS. A 10 μL aliquot of the suspension was mixed with 10 μL Trypan Blue dye (0.4%, Sigma-Aldrich, St. Louis, MO, USA) in a 1:1 ratio, and 10 μL of the mixture was loaded onto a Neubauer hemocytometer for manual counting under a light microscope (Leica DM500, Wetzlar, Germany).

Cell viability was calculated using the formula:

$$\text{Viability (\%)} = \frac{\text{Number of unstained cells}}{\text{Total number of cells}} \times 100$$

4.6. Flow Cytometry for Apoptosis (Annexin V/PI Staining)

Apoptosis was assessed using Annexin V/PI staining followed by flow cytometry to distinguish viable, early apoptotic, late apoptotic, and necrotic cells based on phosphatidylserine externalization and membrane integrity [liii].

LNCaP cells were seeded in 6-well plates at 2×10^5 cells per well in 2 mL of RPMI-1640 medium and allowed to adhere for 24 h at 37°C in a humidified incubator with 5% CO_2 . Cells were then treated with varying concentrations of *J. spicigera* extract (specifically 250, 500, and 1000 $\mu\text{g}/\text{mL}$), with 0.1% DMSO as the vehicle control and 10 μM etoposide (Sigma-Aldrich, St. Louis, MO, USA) as the positive control. Each condition was tested in three independent experiments [li].

Following treatment, cells were harvested by trypsinization (0.25% Trypsin-EDTA, Gibco, Waltham, MA, USA) for 2 min at 37°C , neutralized with RPMI-1640 medium containing 10% FBS, and resuspended in cold PBS. A total of 1×10^5 cells were transferred to fluorescence-activated cell

sorting (FACS) tubes, centrifuged at $300 \times g$ for 5 min, and resuspended in 100 μL of 1X Annexin V binding buffer (BD Biosciences, Franklin Lakes, NJ, USA). Cells were stained with 5 μL of Annexin V-FITC and 5 μL of propidium iodide (PI, 50 $\mu\text{g}/\text{mL}$, BD Biosciences, Franklin Lakes, NJ, USA) and incubated in the dark for 15 min at room temperature.

After incubation, 400 μL of 1X binding buffer was added, and samples were immediately analyzed using a flow cytometer (BD Accuri C6, BD Biosciences, Franklin Lakes, NJ, USA). Data was acquired from at least 10,000 events per sample, and analysis was performed using FlowJo v10 software (BD Biosciences, Franklin Lakes, NJ, USA).

Apoptotic cell populations were classified as: 1) annexin V⁻/PI⁻ for viable cells; 2) annexin V⁺/PI⁻ for early apoptotic cells; 3) annexin V⁺/PI⁺ for late apoptotic cells; and 4) annexin V⁻/PI⁺ for necrotic cells [liii].

4.7. Cell Cycle Analysis (PI Staining by Flow Cytometry)

To evaluate the effects of *J. spicigera* extract on cell cycle progression in LNCaP cells, PI staining followed by flow cytometry was performed. This method quantifies DNA content in individual cells, enabling the identification of G₀/G₁, S, and G₂/M phases, as well as sub-G₀/G₁ populations indicative of apoptotic DNA fragmentation [liv].

LNCaP cells were seeded at 2×10^5 cells per well in 6-well plates containing 2 mL of RPMI-1640 medium and incubated at 37°C with 5% CO₂ for 24 h to allow adherence. Cells were then treated with varying concentrations of *J. spicigera* extract (specifically 250 and 500 $\mu\text{g}/\text{mL}$), with 0.1% DMSO as the vehicle control, 10 μM etoposide (Sigma-Aldrich, St. Louis, MO, USA) and 5-fluorouracil as the positive controls. Each condition was tested in three independent experiments [li,liv].

Following treatment, both floating and adherent cells were collected by trypsinization (0.25% Trypsin-EDTA, Gibco, Waltham, MA, USA) and centrifugation at $300 \times g$ for 5 min at 4°C. The cell pellet was washed twice with cold phosphate-buffered saline (PBS, pH 7.4), resuspended in 500 μL of ice-cold PBS, and fixed by adding 1 mL of 70% ethanol dropwise while vortexing. Fixed cells were stored at -20°C for at least 24 h before further processing.

On the day of analysis, ethanol-fixed cells were centrifuged at $500 \times g$ for 5 min, washed twice with PBS, and incubated with RNase A (100 $\mu\text{g}/\text{mL}$, Sigma-Aldrich, St. Louis, MO, USA) at 37°C for 30 min to eliminate RNA contamination. PI staining was performed by adding 50 $\mu\text{g}/\text{mL}$ propidium iodide (Sigma-Aldrich, St. Louis, MO, USA) in PBS containing 0.1% Triton X-100, followed by incubation for 15 min in the dark at room temperature.

Flow cytometry analysis was conducted using a BD FACSCanto II flow cytometer (BD Biosciences, Franklin Lakes, NJ, USA), acquiring 10,000 events per sample on the FL2-A channel (PI fluorescence at 620 nm). The cell cycle distribution was analyzed using FlowJo v10 software (BD Biosciences, Franklin Lakes, NJ, USA) with the Watson pragmatic cell cycle modeling algorithm to determine the percentage of cells in G₀/G₁, S, and G₂/M phases. The sub-G₀/G₁ population, indicative of apoptotic cells with fragmented DNA, was also quantified [liv].

4.8. Statistical Analysis

All experiments were performed in triplicate across three independent experiments, and data are presented as mean \pm standard error of the mean (SEM). Statistical significance was assessed using one-way ANOVA followed by Tukey's post hoc test, with $p < 0.05$ and $p < 0.001$.

Flow cytometry data were analyzed using FlowJo v10 software (BD Biosciences, Franklin Lakes, NJ, USA), and cell cycle distribution was determined using the Watson pragmatic cell cycle modeling algorithm. All graphs and plots were generated using GraphPad Prism 10.0 (GraphPad Software, San Diego, CA, USA).

5. Conclusions

This study provides the first detailed evidence that a hydroalcoholic extract of *Justicia spicigera* Schltdl. exerts a potent, dose-dependent antiproliferative effect on androgen-sensitive LNCaP

prostate cancer cells. The results establish a dual mechanism of action wherein the extract functions as a cytostatic agent at lower concentrations (250 µg/mL) by inducing significant G₀/G₁ cell cycle arrest, while transitioning to a pro-apoptotic agent at higher concentrations (≥500 µg/mL). Phytochemical profiling suggests that these biological effects may be driven by bioactive flavonoids such as kaempferitrin. Altogether, these results provide a scientific rationale for the traditional use of "muicle" in Mexican ethnomedicine and highlight its potential as a source of novel scaffolds for prostate cancer therapy. By selectively targeting cell cycle checkpoints at sub-lethal doses, *J. spicigera* offers a promising template for developing treatments that could delay tumor progression with potentially lower systemic toxicity than conventional chemotherapeutics. Future research should prioritize the isolation and structural elucidation of the active constituents, alongside *in vivo* studies to confirm their selectivity, safety, and therapeutic efficacy in complex biological systems.

Supplementary Materials: The following supporting information can be downloaded at the website of this paper posted on Preprints.org.

Author Contributions: Conceptualization: M.E.H.-A., F.R.R.-M. and T.J.P.; Methodology: I.B.-E., F.H.-R., M.E.H.-A., M.G.-V. and R.R.R.-H.; Software: R.R.R.-H., S.G.-P. and E.C.-P.; Validation: M.E.H.-A., C.A.L.-R., and E.C.-P.; Formal Analysis: I.B.-E., R.R.R.-H., and T.J.P.; Investigation: I.B.-E., F.H.-R., M.E.H.-A., M.G.-V., R.R.R.-H. and S.G.-P.; Resources: M.E.H.-A., F.R.R.-M. and T.J.P.; Data Curation: I.B.-E. and C.A.L.-R.; Writing—Original Draft Preparation: I.B.-E. R.R.R.-H. and T.J.P.; Writing—Review and Editing: F.R.R.-M., M.E.H.-A., and T.J.P.; Visualization: I.B.-E. and T.J.P.; Supervision: F.R.R.-M. and T.J.P.; Project Administration: F.R.R.-M.; Funding Acquisition: F.H.-R. and F.R.R.-M. All authors have read and agreed to the published version of the manuscript.

Funding: This research received no external funding.

Data Availability Statement: The data produced from this study is available from the corresponding author upon reasonable request. This includes raw flow cytometry files, spectroscopic and chromatographic datasets, and processed quantitative analyses used in the evaluation of cell viability, apoptosis, and phytochemical composition.

Acknowledgments: I. B.-E., C.A.R.-L. and S.G.-P., thanks SECIHTI of Mexico for their Ph.D. scholarship [289304, 744624, and 792984 respectively]. The authors have reviewed and edited the output and take full responsibility for the content of this publication.

Conflicts of Interest: The authors declare no conflicts of interest.

References

- ⁱ Raychaudhuri, R.; Lin, D.W.; Montgomery, R.B. Prostate Cancer: A Review. *JAMA* **2025**, *333*, 1433–1446. <https://doi.org/10.1001/jama.2025.0228>
- ⁱⁱ Mignozzi, S.; Santucci, C.; Levi, F.; Malvezzi, M.; Boffetta, P.; Corso, G.; Negri, E.; La Vecchia, C. Cancer mortality predictions for 2025 in Latin America with focus on prostate cancer. *Eur. J. Cancer Prev.* **2025**, doi:10.1097/CEJ.0000000000000959.
- ⁱⁱⁱ Ferlay, J.; Colombet, M.; Soerjomataram, I.; Parkin, D.M.; Piñeros, M.; Znaor, A.; Bray, F. Cancer statistics for the year 2020: An overview. *Int. J. Cancer* **2021**, *149*, 778–789. <https://doi.org/10.1002/ijc.33588>
- ^{iv} INEGI. *Defunciones registradas de hombres por tumor maligno de la próstata por entidad federativa de residencia habitual y grupo quinquenal de edad, serie 2010 a 2023*; Instituto Nacional de Estadística, Geografía e Informática: Aguascalientes, Mexico, 2025. Available online: <https://www.inegi.org.mx/app/tabulados/interactivos/?pxq=mortalidad> (accessed on 20 January 2026).

- ^v SSA. *Boletín Epidemiológico. Sistema Nacional de Vigilancia Epidemiológica. Sistema Único de Información*; Dirección General de Epidemiología, Secretaría de Salud: Mexico City, Mexico, 2025; Volume 42, No. 1. Available online: <https://www.gob.mx/salud/acciones-y-programas/direccion-general-de-epidemiologia-boletin-epidemiologico> (accessed on 20 January 2026).
- ^{vi} Sekhoacha, M.; Riet, K.; Motloun, P.; Gumenku, L.; Adegoke, A.; Mashele, S. Prostate Cancer Review: Genetics, Diagnosis, Treatment Options, and Alternative Approaches. *Molecules* **2022**, *27*, 5730. <https://doi.org/10.3390/molecules27175730>
- ^{vii} Lowrance, W.; Dreicer, R.; Jarrard, D.F.; Scarpato, K.R.; Kim, S.K.; Kirkby, E.; Cookson, M.S. Updates to Advanced Prostate Cancer: AUA/SUO Guideline (2023). *J. Urol.* **2023**, *209*, 1082–1090. <https://doi.org/10.1097/JU.0000000000003452>
- ^{viii} Rodriguez-Canales, M.; Jimenez-Rivas, R.; Canales-Martinez, M.M.; Garcia-Lopez, A.J.; Rivera-Yanez, N.; Nieto-Yanez, O.; Rodriguez-Monroy, M.A. Protective Effect of *Amphipterygium adstringens* Extract on Dextran Sulphate Sodium-Induced Ulcerative Colitis in Mice. *Mediators Inflamm.* **2016**, *2016*, 8543561. <https://doi.org/10.1155/2016/8543561>
- ^{ix} Rojas-Armas, J.P.; Arroyo-Acevedo, J.L.; Palomino-Pacheco, M.; Ortiz-Sanchez, J.M.; Calva, J.; Justil-Guerrero, H.J.; Herrera-Calderon, O. Phytochemical Constituents and Ameliorative Effect of the Essential Oil from *Annona muricata* L. Leaves in a Murine Model of Breast Cancer. *Molecules* **2022**, *27*, 1818. <https://doi.org/10.3390/molecules27061818>
- ^x López-Rosas, C.A.; González-Periañez, S.; Pawar, T.J.; Zurutuza-Lorméndez, J.I.; Ramos-Morales, F.R.; Olivares-Romero, J.L.; Saavedra Vélez, M.V.; Hernández-Rosas, F. Anticonvulsant Potential and Toxicological Profile of *Verbesina persicifolia* Leaf Extracts: Evaluation in Zebrafish Seizure and *Artemia salina* Toxicity Models. *Plants* **2025**, *14*, 1078. <https://doi.org/10.3390/plants14071078>
- ^{xi} Ventura-Hernández, K. I.; Pawar, T. J.; Ramos-Morales, F. R.; López-Rosas, C. A.; Hernández-Rosas, F. Chemical Duality of *Verbesina* Metabolites: Sesquiterpene Lactones, Selectivity Index (SI), and Translational Feasibility for Anti-Resistance Drug Discovery. *Preprints* **2026**, 2026011104. <https://doi.org/10.20944/preprints202601.1104.v1>
- ^{xii} Sofi, F.A.; Tabassum, N. Natural product inspired leads in the discovery of anticancer agents: an update. *J. Biomol. Struct. Dyn.* **2023**, *41*, 8605–8628. <https://doi.org/10.1080/07391102.2022.2134212>
- ^{xiii} Angeles-Lopez, G.E.; Gonzalez-Trujano, M.E.; Rodriguez, R.; Deciga-Campos, M.; Brindis, F.; Ventura-Martinez, R. Gastrointestinal activity of *Justicia spicigera* Schltdl. in experimental models. *Nat. Prod. Res.* **2021**, *35*, 1847–1851. <https://doi.org/10.1080/14786419.2019.1637873>
- ^{xiv} Carneiro, M.R.B.; Sallum, L.O.; Martins, J.L.R.; Peixoto, J.C.; Napolitano, H.B.; Rosseto, L.P. Overview of the *Justicia* Genus: Insights into Its Chemical Diversity and Biological Potential. *Molecules* **2023**, *28*, 1190. <https://doi.org/10.3390/molecules28031190>
- ^{xv} De La Cruz-Jimenez, L.; Hernandez-Torres, M.A.; Monroy-Garcia, I.N.; Rivas-Morales, C.; Verde-Star, M.J.; Gonzalez-Villasana, V.; Viveros-Valdez, E. Biological Activities of Seven Medicinal Plants Used in Chiapas, Mexico. *Plants* **2022**, *11*, 1910. <https://doi.org/10.3390/plants11141910>
- ^{xvi} Castro-Muñoz, R.; León-Becerril, E.; García-Depraect, O. Beyond the Exploration of Muicle (*Justicia spicigera*): Reviewing Its Biological Properties, Bioactive Molecules and Materials Chemistry. *Processes* **2022**, *10*, 1035. <https://doi.org/10.3390/pr10051035>
- ^{xvii} Murillo-Villicana, M.; Noriega-Cisneros, R.; Pena-Montes, D.J.; Huerta-Cervantes, M.; Aguilera-Mendez, A.; Cortes-Rojo, C.; Saavedra-Molina, A. Antilipidemic and Hepatoprotective Effects of Ethanol Extract of *Justicia spicigera* in Streptozotocin Diabetic Rats. *Nutrients* **2022**, *14*, 1946. <https://doi.org/10.3390/nu14091946>

- ^{xviii} Rodríguez-Garza, N.E.; Quintanilla-Licea, R.; Romo-Saenz, C.I.; Elizondo-Luevano, J.H.; Tamez-Guerra, P.; Rodríguez-Padilla, C.; Gómez-Flores, R. *In Vitro* Biological Activity and Lymphoma Cell Growth Inhibition by Selected Mexican Medicinal Plants. *Life* **2023**, *13*, 958. <https://doi.org/10.3390/life13040958>
- ^{xix} Ortiz-Andrade, R.; Cabanas-Wuan, A.; Arana-Argaez, V.E.; Alonso-Castro, A.J.; Zapata-Bustos, R.; Salazar-Olivo, L.A.; García-Carranca, A. Antidiabetic effects of *Justicia spicigera* Schltldl (Acanthaceae). *J. Ethnopharmacol.* **2012**, *143*, 455–462. <https://doi.org/10.1016/j.jep.2012.06.043>
- ^{xx} Pérez-Vasquez, A.; Díaz-Rojas, M.; Castillejos-Ramírez, E.V.; Pérez-Esquivel, A.; Montano-Cruz, Y.; Rivero-Cruz, I.; Mata, R. Protein tyrosine phosphatase 1B inhibitory activity of compounds from *Justicia spicigera* (Acanthaceae). *Phytochemistry* **2022**, *203*, 113410. <https://doi.org/10.1016/j.phytochem.2022.113410>
- ^{xxi} Arberet, L.; Pottier, F.; Michelin, A.; Nowik, W.; Bellot-Gurlet, L.; Andraud, C. Spectral characterisation of a traditional Mesoamerican dye: relationship between in situ identification on the 16th century Codex Borbonicus manuscript and composition of *Justicia spicigera* plant extract. *Analyst* **2021**, *146*, 2520–2530. <https://doi.org/10.1039/d1an00113b>
- ^{xxii} Domínguez, X.A.; Aguilar, H.; González, C.; Ferreé-D'Amare, A.R. Estudio químico del "muitle" (*Justicia spicigera*). *Rev. Latinoamer. Quím.* **1990**, *21*, 142–143.
- ^{xxiii} Euler, K.L.; Alam, M. Isolation of Kaempferitrin From *Justicia spicigera*. *J. Nat. Prod.* **1982**, *45*, 220–221. <https://doi.org/10.1021/np50020a020>
- ^{xxiv} Zapata-Morales, J.R.; Alonso-Castro, A.J.; González-Rivera, M.L.; González Prado, H.I.; Barragan-Galvez, J.C.; Hernández-Flores, A.; Ramírez-Morales, M.A. Synergistic Interaction Between *Justicia spicigera* Extract and Analgesics on the Formalin Test in Rats. *Pharmaceuticals* **2025**, *18*, 187. <https://doi.org/10.3390/ph18020187>
- ^{xxv} Awad, N.E.; Abdelkawy, M.A.; Abdel Rahman, E.H.; Hamed, M.A.; Ramadan, N.S. Phytochemical and *in vitro* Screening of *Justicia spicigera* Ethanol Extract for Antioxidant Activity and *in vivo* Assessment Against *Schistosoma mansoni* Infection in Mice. *Anti-Infective Agents* **2018**, *16*, 49–56. <https://doi.org/10.2174/2211352516666180126161247>
- ^{xxvi} Shahzad, N.; Khan, W.; Md, S.; Ali, A.; Saluja, S.S.; Sharma, S.; Al-Ghamdi, S.S. Phytosterols as a natural anticancer agent: Current status and future perspective. *Biomed. Pharmacother.* **2017**, *88*, 786–794. <https://doi.org/10.1016/j.biopha.2017.01.068>
- ^{xxvii} Cáceres-Cortés, J.R.; Cantu-Garza, F.A.; Mendoza-Mata, M.T.; Chávez-González, M.A.; Ramos-Mandujano, G.; Zambrano-Ramírez, I.R. Cytotoxic activity of *Justicia spicigera* is inhibited by bcl-2 proto-oncogene and induces apoptosis in a cell cycle dependent fashion. *Phytother. Res.* **2001**, *15*, 691–697. <https://doi.org/10.1002/ptr.791>
- ^{xxviii} Vega-Avila, E.; Tapia-Aguilar, R.; Reyes-Chilpa, R.; Guzmán-Gutiérrez, S.L.; Pérez-Flores, J.; Velasco-Lezama, R. Actividad antibacteriana y antifúngica de *Justicia spicigera*. *Rev. Latinoam. Quím.* **2012**, *40*, 75–82.
- ^{xxix} Jacobo-Salcedo, M.d.R.; Alonso-Castro, A.J.; Salazar-Olivo, L.A.; Carranza-Alvarez, C.; González-Espíndola, L.Á.; Domínguez, F.; García-Carranca, A. Antimicrobial and Cytotoxic Effects of Mexican Medicinal Plants. *Nat. Prod. Commun.* **2011**, *6*, 1934578X1100601234. <https://doi.org/10.1177/1934578x1100601234>
- ^{xxx} Juárez-Vázquez, M.C.; Alonso-Castro, A.J.; García-Carranca, A. Kaempferitrin induces immunostimulatory effects in vitro. *J. Ethnopharmacol.* **2013**, *148*, 337–340. <https://doi.org/10.1016/j.jep.2013.03.072>

- xxxi Lowrance, W.; Dreicer, R.; Jarrard, D.F.; Scarpato, K.R.; Kim, S.K.; Kirkby, E.; Cookson, M.S. Updates to Advanced Prostate Cancer: AUA/SUO Guideline (2023). *J. Urol.* **2023**, *209*, 1082–1090. <https://doi.org/10.1097/JU.0000000000003452>
- xxxii Korn, E.L.; Arbuck, S.G.; Pluda, J.M.; Simon, R.; Kaplan, R.S.; Christian, M.C. Clinical trial designs for cytostatic agents: are new approaches needed? *J. Clin. Oncol.* **2001**, *19*, 265–272. <https://doi.org/10.1200/JCO.2001.19.1.265>
- xxxiii Fernández-Pomares, C.; Juárez-Aguilar, E.; Domínguez-Ortiz, M.Á.; Gallegos-Estudillo, J.; Herrera-Covarrubias, D.; Sánchez-Medina, A.; Hernández, M.E. Hydroalcoholic extract of the widely used Mexican plant *Justicia spicigera* Schlttdl. exerts a cytostatic effect on LNCaP prostate cancer cells. *J. Herb. Med.* **2018**, *12*, 66–72. <https://doi.org/10.1016/j.hermed.2017.09.003>
- xxxiv Alonso-Castro, A.J.; Ortiz-Sanchez, E.; Garcia-Regalado, A.; Ruiz, G.; Nunez-Martinez, J.M.; Gonzalez-Sanchez, I.; Garcia-Carranca, A. Kaempferitrin induces apoptosis via intrinsic pathway in HeLa cells and exerts antitumor effects. *J. Ethnopharmacol.* **2013**, *145*, 476–489. <https://doi.org/10.1016/j.jep.2012.11.016>
- xxxv Shi, Z.; Shen, Y.; Liu, X.; Zhang, S. Kaempferitrin Regulates the Proliferation, Metastasis, and Immune Escape of Nonsmall Cell Lung Cancer by Inhibiting the Akt/NF-κB Pathway. *Drug Dev. Res.* **2025**, *86*, e70117. <https://doi.org/10.1002/ddr.70117>
- xxxvi Kopustinskiene, D.M.; Jakstas, V.; Savickas, A.; Bernatoniene, J. Flavonoids as Anticancer Agents. *Nutrients* **2020**, *12*, 457. <https://doi.org/10.3390/nu12020457>
- xxxvii Rahman, N.; Khan, H.; Zia, A.; Khan, A.; Fakhri, S.; Aschner, M.; Saso, L. Bcl-2 Modulation in p53 Signaling Pathway by Flavonoids: A Potential Strategy towards the Treatment of Cancer. *Int. J. Mol. Sci.* **2021**, *22*, 11315. <https://doi.org/10.3390/ijms222111315>
- xxxviii Chen, Y.; He, S.; Zeng, A.; He, S.; Jin, X.; Li, C.; Lu, Q. Inhibitory Effect of β-Sitosterol on the Ang II-Induced Proliferation of A7r5 Aortic Smooth Muscle Cells. *Anal. Cell. Pathol. (Amst)* **2023**, *2023*, 2677020. <https://doi.org/10.1155/2023/2677020>
- xxxix Elasbali, A.M.; Al-Soud, W.A.; Al-Oanzi, Z.H.; Qanash, H.; Alharbi, B.; Binsaleh, N.K.; Adnan, M. Cytotoxic Activity, Cell Cycle Inhibition, and Apoptosis-Inducing Potential of *Athyrium hohenackerianum* (Lady Fern) with Its Phytochemical Profiling. *Evid. Based Complement. Alternat. Med.* **2022**, *2022*, 2055773. <https://doi.org/10.1155/2022/2055773>
- xl Jia, X.B.; Zhang, Q.; Xu, L.; Yao, W.J.; Wei, L. Lotus leaf flavonoids induce apoptosis of human lung cancer A549 cells through the ROS/p38 MAPK pathway. *Biol. Res.* **2021**, *54*, 7. <https://doi.org/10.1186/s40659-021-00330-w>
- xli Jomova, K.; Alomar, S.Y.; Valko, R.; Liska, J.; Nepovimova, E.; Kuca, K.; Valko, M. Flavonoids and their role in oxidative stress, inflammation, and human diseases. *Chem. Biol. Interact.* **2025**, *413*, 111489. <https://doi.org/10.1016/j.cbi.2025.111489>
- xlii Lin, F.; Xu, L.; Huang, M.; Deng, B.; Zhang, W.; Zeng, Z.; Yinzhi, S. β-Sitosterol Protects against Myocardial Ischemia/Reperfusion Injury via Targeting PPARγ/NF-κB Signalling. *Evid. Based Complement. Alternat. Med.* **2020**, *2020*, 2679409. <https://doi.org/10.1155/2020/2679409>
- xliiii Su, M.; Li, Z.; Zhou, S.; Zhang, H.; Xiao, Y.; Li, W.; Li, J. Kaempferitrin, a major compound from ethanol extract of *Chenopodium ambrosioides*, exerts antitumour and hepatoprotective effects in the mice model of human liver cancer xenografts. *J. Pharm. Pharmacol.* **2023**, *75*, 1066–1075. <https://doi.org/10.1093/jpp/rgad046>
- xliv Wong, S.C.; Kamarudin, M.N.A.; Naidu, R. Anticancer Mechanism of Flavonoids on High-Grade Adult-Type Diffuse Gliomas. *Nutrients* **2023**, *15*, 797. <https://doi.org/10.3390/nu15040797>

-
- ^{xlv} Zhou, S.; Zhang, H.; Li, J.; Li, W.; Su, M.; Ren, Y.; Shang, H. Potential anti-liver cancer targets and mechanisms of kaempferitrin based on network pharmacology, molecular docking and experimental verification. *Comput. Biol. Med.* **2024**, *178*, 108693. <https://doi.org/10.1016/j.compbiomed.2024.108693>
- ^{xlvi} Zhu, X.; Pan, Y.; Xu, X.; Xu, J. Kaempferitrin alleviates LPS-induced septic acute lung injury in mice through downregulating NF- κ B pathway. *Allergol. Immunopathol. (Madr)*. **2023**, *51*, 1–7. <https://doi.org/10.15586/aei.v51i6.838>
- ^{xlvii} Shankar, S.; Srivastava, R.K. Bax and Bak genes are essential for maximum apoptotic response by curcumin, a polyphenolic compound and cancer chemopreventive agent derived from turmeric, *Curcuma longa*. *Carcinogenesis* **2007**, *28*, 1277–1286. <https://doi.org/10.1093/carcin/bgm024>
- ^{xlviii} Hsieh, T.C.; Wu, J.M. Differential effects on growth, cell cycle arrest, and induction of apoptosis by resveratrol in human prostate cancer cell lines. *Exp. Cell Res.* **1999**, *249*, 109–115. <https://doi.org/10.1006/excr.1999.4471>
- ^{xlix} Pilling, A.; Kim, S.H.; Hwang, C. Androgen receptor negatively regulates mitotic checkpoint signaling to induce docetaxel resistance in castration-resistant prostate cancer. *Prostate* **2022**, *82*, 182–192. <https://doi.org/10.1002/pros.24257>
- ^l van Meerloo, J.; Kaspers, G.J.; Cloos, J. Cell sensitivity assays: the MTT assay. *Methods Mol. Biol.* **2011**, *731*, 237–245. https://doi.org/10.1007/978-1-61779-080-5_20
- ^{li} Wang, H.; Wei, X.; Zhang, D.; Li, W.; Hu, Y. LNCaP-AI prostate cancer cell line establishment by Flutamide and androgen-free environment to promote cell adherent. *BMC Mol. Cell Biol.* **2022**, *23*, 51. <https://doi.org/10.1186/s12860-022-00453-2>
- ^{lii} Strober, W. Trypan Blue Exclusion Test of Cell Viability. *Curr. Protoc. Immunol.* **2015**, *111*, A3.B.1–A3.B.3. <https://doi.org/10.1002/0471142735.ima03bs111>
- ^{liii} Lakshmanan, I.; Batra, S.K. Protocol for Apoptosis Assay by Flow Cytometry Using Annexin V Staining Method. *Bio Protoc.* **2013**, *3*, e374. <https://doi.org/10.21769/bioprotoc.374>
- ^{liv} Kim, K.H.; Sederstrom, J.M. Assaying Cell Cycle Status Using Flow Cytometry. *Curr. Protoc. Mol. Biol.* **2015**, *111*, 28.6.1–28.6.11. <https://doi.org/10.1002/0471142727.mb2806s111>